In-Situ Formation of Sandwiched Structures of Nanotube/Cu_xO_y/Cu Composites for Lithium Battery Applications

Subramanian Venkatachalam,[†] Hongwei Zhu,[†] Charan Masarapu,[†] KaiHsuan Hung,[†] Z. Liu,[‡] K. Suenaga,[‡] and Bingqing Wei[†,*]

[†]Department of Mechanical Engineering, University of Delaware, Newark, Delaware 19716, and [‡]AIST, Research Center for Advance Carbon Materials, Tsukuba, Ibaraki 3058565, Japan

ABSTRACT Development of materials and structures leading to lithium ion batteries with high energy and power density is a major requirement for catering to the power needs of present day electronic industry. Here, we report an *in situ* formation of a sandwiched structure involving single-walled carbon nanotube film, copper oxide, and copper during the direct synthesis of nanotube macrofilms over copper foils and their electrochemical performance in lithium ion batteries. The sandwiched structure showed a remarkably high reversible capacity of 220 mAh/g at a high cycling current of 18.6 A/g (50 C), leading to a significantly improved electrochemical performance which is extremely high compared to pure carbon nanotube and any other carbon based materials.

KEYWORDS: lithium ion battery · single-walled carbon nanotube · copper oxide · composite · sandwiched structures · anode material

Increase in demand for a reliable, quickly rechargeable power source has been on a constant rise because of the growing portable electronics market and catering to the power needs of electric vehicle development.[1] The lithium ion battery is one of the most promising power sources that can satisfy this ever growing demand.[2,3] In recent years, utilizing nanostructured materials as electrodes in lithium ion batteries have shown enormous promise with respect to both energy density and power density of the battery.[4,5] The critical parameters that have to be focused for improving the energy density and the power density of lithium ion battery are the ability to insert and remove Li ions at high currents without compromising much on the specific capacity of the chosen material. Intercalation anodes based on graphite are presently used as anode materials;[6] however, the main limitation of graphitic anode is its specific capacity (372 mAh/g). Disordered carbons with huge reversible and irreversible capacities have been reported extensively.[7] Alternative anodes such as metal oxides[8,9] are also under close scrutiny, however, the problems such as electronic conductivity and volume expansion during Li topotactic process forces such materials away from being commercially exploited.

Carbon nanotubes (CNTs) are an interesting class of materials that are finding applications in variety of fields ranging from biology to space science because of their interesting electrical, thermal, and mechanical properties. Lithium insertion reactions have been reported in both single-walled carbon nanotubes (SWNTs) and multiwalled carbon nanotubes (MWNTs).[10−13] However, no earlier reports have dealt in depth on the current capability of such anode materials in lithium ion battery which is crucial for high performance lithium ion batteries. Although ideal CNTs are considered as the rolling of individual graphene sheets, it is actually a mixture of graphite and disordered carbon structures because of the existence of different defects in CNTs. A variety of pore structure, size, and geometry exists depending on the number of CNT bundles and their arrangements. Hence, the expected specific capacity is comparatively larger than pure graphite.

In this report, we present a novel and simple sandwiched composite structures based on SWNT macrofilm as an anode material that showed both high energy and power densities. We have succeeded in preparing macrofilms of SWNTs *in situ* on various substrates by applying a liquid-free precursor system.[14] Advantages of considering nanotube films for these applications are their uniform dimensions, large specific surface area, and smooth surface topology. In

*Address correspondence to weib@udel.edu.

Received for review April 29, 2009 and accepted July 21, 2009.

Published online July 28, 2009.
10.1021/nn900432u CCC: $40.75

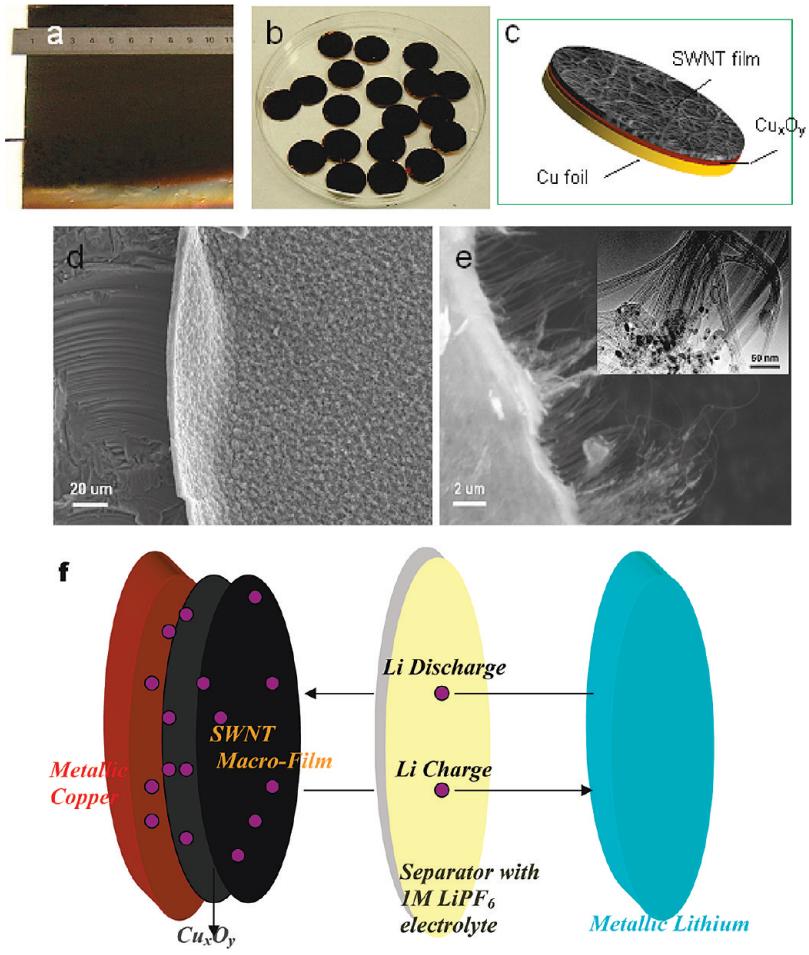

Figure 1. Fabrication of sandwiched Cu/Cu_xO_y/SWNT composites as anode materials: (a) photograph of SWNT film deposited on Cu foil; (b) electrodes punched from the deposited film on Cu substrate; (c) a schematic illustration of the Cu/Cu_xO_y/SWNT sandwiched structure; (d) low resolution SEM image, revealing the film integrity and its isotropic morphology; (e) high resolution SEM and TEM (inset) of the SWNTs. Most of SWNTs were observed as bundles with 20−100 nm thickness; (f) schematics of a Cu/Cu_xO_y/SWNT film sandwiched structure electrode in a lithium half-cell configuration.

this study, electrodes for a lithium ion battery were fabricated by depositing SWNT macrofilms directly on copper foils, followed by a simple postpunching process (Figure 1). Both SEM and TEM characterizations suggest that the SWNT macrofilms are composed of entangled SWNT bundles and a certain amount of impurities, including amorphous carbon and catalytic iron nanoparticles of about ~30% based on EDX results (not shown in Figure 1). The SWNT macrofilm possesses a perfect structural uniformity and good adhesion with the Cu-foil substrate (Figure 1b,d) which is used as a current collector in the lithium ion battery system. It is worth noting that a thin layer of copper oxide, which has been confirmed by XPS measurements (Supporting Information, Figure S1), was formed at the SWNT−Cu interface during the direct deposition process, leading to the formation of a sandwiched structure involving metallic copper, copper oxide, and SWNT film as schematized in Figure 1c. A typical schematic of the Cu/Cu_xO_y/SWNT film sandwiched structure in a half cell configuration across Li metal is shown in Figure 1f.

The as prepared Cu/Cu_xO_y/SWNT sandwiched structures were studied for their electrochemical performance by assembling two electrode test cells with Li metal as a reference and counter-electrode in a 1 M $LiPF_6$ in EC:DEC electrolyte and the details are described elsewhere.[15] For comparison, the electrodes were assembled in four different configurations: SWNT macrofilms deposited directly on Cu foil inside the CVD reactor, that is, *in situ* formation of the Cu/Cu_xO_y/SWNT sandwiched structures (case 1); SWNT macrofilms deposited on unheated Cu foil outside the CVD reactor, that is, Cu/SWNT structures without the copper oxide layer (case 2); purified SWNT macrofilms deposited outside on a heated Cu foil, that is, Cu/Cu_xO_y/SWNT sandwiched structures without Fe catalysts (case 3); and a heated Cu foil without SWNT macrofilm deposition, that is, only the Cu/Cu_xO_y formation (case 4). Details of case 3 and case 4 can be found in the Supporting Information.

The typical first and second galvanostatic charge−discharge cycle curves are shown in Figure 2a,b for the SWNT film deposited inside (case 1) and outside (case 2) the CVD reactor on Cu foil, respectively. In case 1, the weight of the SWNT film including the iron catalyst particles is considered while calculating the specific capacity of the battery (see Methods sections for estimating the active electrode weight). It can be seen from Figure 2a that during the lithium insertion (discharge) in the first cycle, apart from the typical irreversible film formation reaction at 0.8−0.9 V, which is limited to the first cycle lithium insertion (discharge) and prevents further reaction between the electrode surface and the electrolyte and any electron tunneling,[16] the charge−discharge curves have one interestingly new electrochemical behavior which is not a fingerprint of any carbonaceous material. The differential capacity plots shown as insets of Figure 2a clearly show the reversible peaks at ~1.8 V. Cyclic voltammetry (CV) is an effective technique to monitor the minute electrochemical reactions associated with any system and the first two cycles for the case 1 are shown in Figure 2c,d. The CV results complement the differential capacity plots of the charge−discharge curves. The reversible peaks are not limited to the first cycle and can be seen in the second cycle and following cycles as well. Such a behavior could be attributed to the resulted copper/copper oxide/SWNT sandwiched

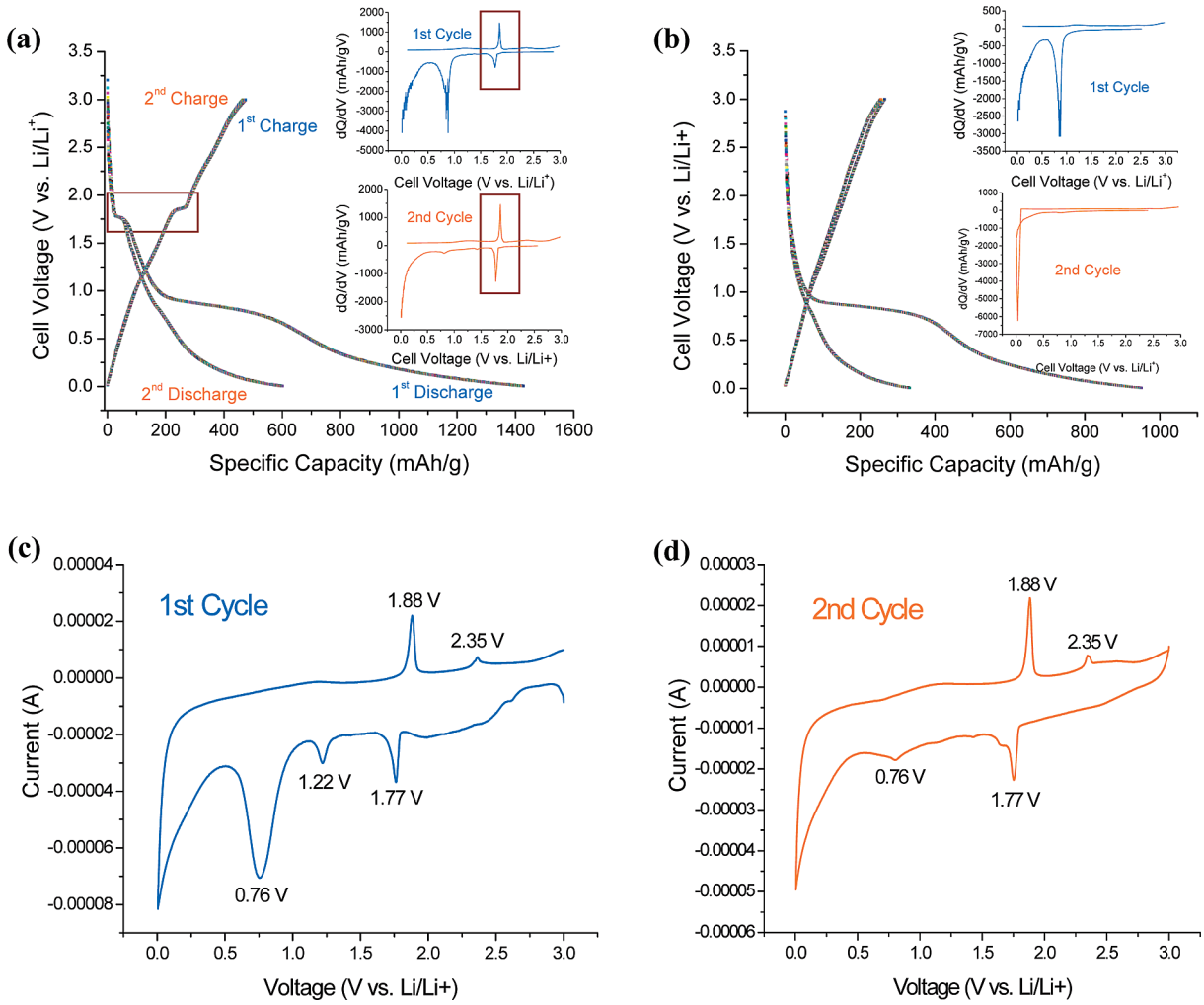

Figure 2. Charge−discharge profiles and cyclic voltammograms: (a) SWNT film deposited on Cu foil inside the CVD reactor (case 1), cycled at 0.2 C rate; (b) SWNT film deposited outside the CVD reactor (case 2), cycled at 0.2 C rate. The insets in panels a and b show the differential capacity plots of the 1st and 2nd cycle. The box in panel a indicates the electrochemical reaction arising from Cu_xO_y. The cycling was performed in a two electrode cell with lithium metal as an anode in a 1 M $LiPF_6$:EC:DEC electrolyte. (c,d) First and second cyclic voltammetry profiles of the battery with the Cu/Cu_xO_y/SWNT sandwiched structure electrode at 0.05 mV/s scan rate.

structures which have electrochemically active copper oxide species coexisting with the SWNT film at the interface between the Cu foil and the SWNT macrofilm.

The charge−discharge curves of the case 2 were akin to that of SWNT film deposited inside CVD reactor (case 1) except for the absence of the reversible reaction at ~1.8 V as shown in Figure 2b. Hence, the electrochemical redox process during the lithium topotactic reactions must be because of the existence of an electrochemically active copper oxide formed *in situ* during the SWNT macrofilm deposition process. It has to be noted that the catalyst iron nanoparticles present in the SWNT macrofilm did not have any electrochemical activity. To verify this, purified SWNT macrofilm where all iron nanoparticles were thoroughly removed from the SWNT film by a chemical process,[17] was deposited on a heat-treated Cu foil (case 3) and its electrochemical behavior is shown in the Supporting Information (Figure S2). The profiles of the charge−discharge curves are similar to that of the case 1, confirming the inactivity of the iron nanoparticles and the important role of copper oxide in the overall electrochemical reactions. To confirm the presence of copper oxide, a Cu foil was heated under the same CVD conditions as the SWNT growth but without any chemical flow and the electrochemical performance was tested (case 4). The surface of the heated Cu foil was confirmed to have a layer of copper oxide as shown by XPS measurements (see Supporting Information, Figure S1). The reversible reaction at ~1.8 V (Figure S3) is also consistent with literature reported on copper oxides.[18−22]

The cycling performance of the Cu/Cu_xO_y/SWNT sandwiched structure (case 1) and the simple Cu/SWNT structure (case 2) across Li metal is shown in Figure 3. The most important observation is the difference in the specific capacity, cycling stability, and rate capability in both cases. It is obvious that the Cu/Cu_xO_y/SWNT sandwiched structure that has the copper oxide layer at the interface is showing both higher specific capacity and cycling efficiency for all charge−discharge rates

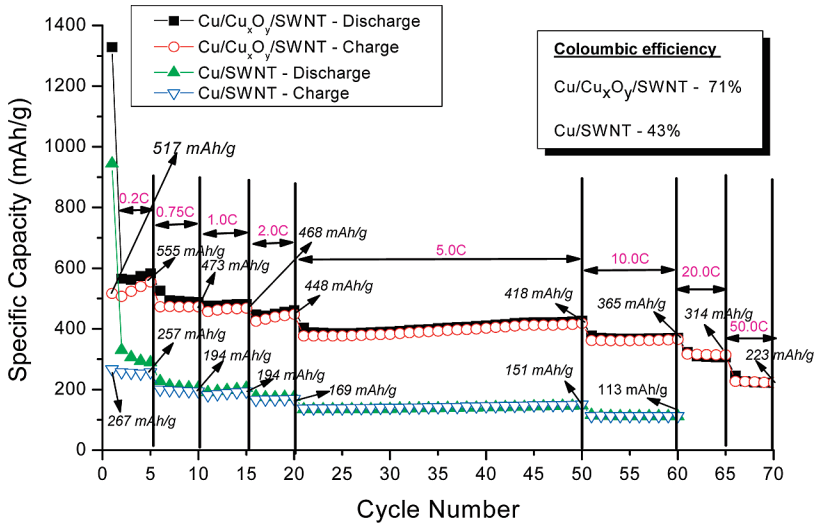

Figure 3. Comparison of the charge−discharge performance of the batteries with the Cu/Cu$_x$O$_y$/SWNT sandwiched structure as electrode and the Cu/SWNT film electrode. The battery with Cu/Cu$_x$O$_y$/SWNT sandwiched structure as an electrode has better performance compared to the battery with the Cu/SWNT film electrode, with a value of about 220 mAh/g even at a rate of 50 C.

studied from 0.2 to 50 C. There is more than a double the capacity for the Cu/Cu$_x$O$_y$/SWNT sandwiched system when compared to that of the Cu/SWNT system as shown in Figure 3. Also, the overall cycling efficiency for the Cu/Cu$_x$O$_y$/SWNT sandwiched system was 71% while that for the Cu/SWNT film system is only 43%. In fact, the cell performance was dropped to very low values for the Cu/SWNT film system when cycled at 50 C rate. However, the Cu/Cu$_x$O$_y$/SWNT sandwiched structure showed excellent capacity and stability even when cycled at a very high rate of 50 C (current density of 18.6 A/g). The specific capacity was ~ 220 mAh/g at 50 C, which is the best reported value for any carbonaceous materials to the best of our knowledge. This is a very important finding that can be considered as door opening phenomena in lithium battery based electrode materials. An earlier work involving CuO and CNTs composite has reported a very fast fading in capacity even at low cycling rate (20 mA/g) which has been attributed to the exfoliation process[23] happening in CNT with an EC based electrolyte. Based on the above result the existence of composite is not the only primary factor for the improved electrochemical performance, instead, the presence of the composite in a sandwiched structure involving metallic copper, copper oxide and SWNT film is imperative for an enhanced energy and power density of the lithium ion battery. The concept of sandwich structured electrode presented here may result in a series of composites in a sandwich configuration involving other metal oxides and SWNT film on a current collector. It is not necessary to have an *in situ* formation of a metallic oxide, instead, formation of a metal oxide thin film over metallic copper by sputtering technique and subsequent deposition of SWNT films is also expected to show enhanced electrochemical performance.

There has been different point of views on the electrochemical reactions of copper oxide with lithium.[18−22] The overall reaction between copper oxide and Li is[19,20]

$$CuO + 2Li \leftrightarrow Li_2O + Cu.$$

The reaction observed in the cathodic region of the first CV plot (Figure 2c,d) for the SWNT macrofilm deposited inside the CVD reactor shows three distinct peaks at 1.77, 1.22, and 0.76 V while in the anodic region two peaks are observed at 1.88 and 2.35 V. The CV profile for the SWNT or any carbonaceous material is completely different from what has been observed in the present case except for the surface film formation reaction at ~0.76 V. The additional peaks observed in the CV curves indicate a multistep electrochemical reaction which is reversible in all the following cycles (for instance see Figure 2d) and mainly due to the presence of copper oxide at the Cu/SWNT macrofilm interface. The heated Cu foil which was confirmed to have a layer of copper oxide by XPS showed exactly same redox peaks (Figure S3) as observed for the SWNT macrofilm deposited inside the CVD reactor. From above observations it is explicit that the main improvement in the electrochemical performance for the SWNT macrofilm deposited inside the CVD reactor (case 1) when compared to that deposited outside (case 2) is mainly due to the existence of copper oxide at the interface.

To see the effect of copper oxide in the electrochemical reactions, the cycled electrodes were studied using HRTEM and EELS. Here, we have chosen the purified SWNT electrode (case 3) in order to avoid any influence of the Fe nanoparticles which coexist in the unpurified SWNT macrofilm (case 1). The HRTEM examination was performed (1) after one complete discharge (full Li insertion) and (2) after one complete cycle (full Li deinsertion). The typical HRTEM and the SAED patterns are shown in Figure 4a,b. A significant percentage of predominantly Cu nanoparticles are found in the SWNT film after the first discharge, as shown in Figure 4a. It is clear from the SAED pattern that the Cu nanoparticles are uniform crystalline in size from 3 to 10 nm and have been indexed as fcc structure. Figure 4b confirms the formation of Cu_2O (a mixture of *Pn*3 and *Pn*3*m*) after one complete cycle. EELS measurements (not shown here) also showed the presence of Cu nanoparticles after one discharge and the copper oxide after one complete cycle. These studies further confirm the role of copper oxide in the improved electrochemical performance of the Cu/Cu$_x$O$_y$/SWNT sandwiched structure as a lithium battery anode material.

On the basis of the results of the HRTEM and SAED, the enhanced diffusion of Li ions in the Cu/Cu_xO_y/SWNT sandwiched composite system can be explained with the schematics representing changes in the electrode at the end of the first charge and discharge cycle as shown in Figure 4c. The Li insertion reaction into the copper oxide layer resulted in the formation of Cu nanoparticles which migrated into the SWNT bundles with the flooding of the electrolyte. This has resulted in the presence of Cu nanoparticles at the interface of the electrode and electrolyte which greatly improves the electronic property of the system. In other words, the presence of copper oxide has played a role as a catalyst in increasing the Li ion transfer rate across the electrode−electrolyte interface. An increase in the Li ion transfer rate implies a significant reduction in the activation energy required for the Li ion migration across the electrode−electrolyte interface as proposed by Huang *et al.*,[24] which is very critical for the high rate capability of the Cu/Cu_xO_y/SWNT electrode system. The process of copper oxide converting into copper repeats in every subsequent charge−discharge cycles thus giving superior performance of the battery with the Cu/Cu_xO_y/SWNT electrode compared to the one with the Cu/SWNT electrode.

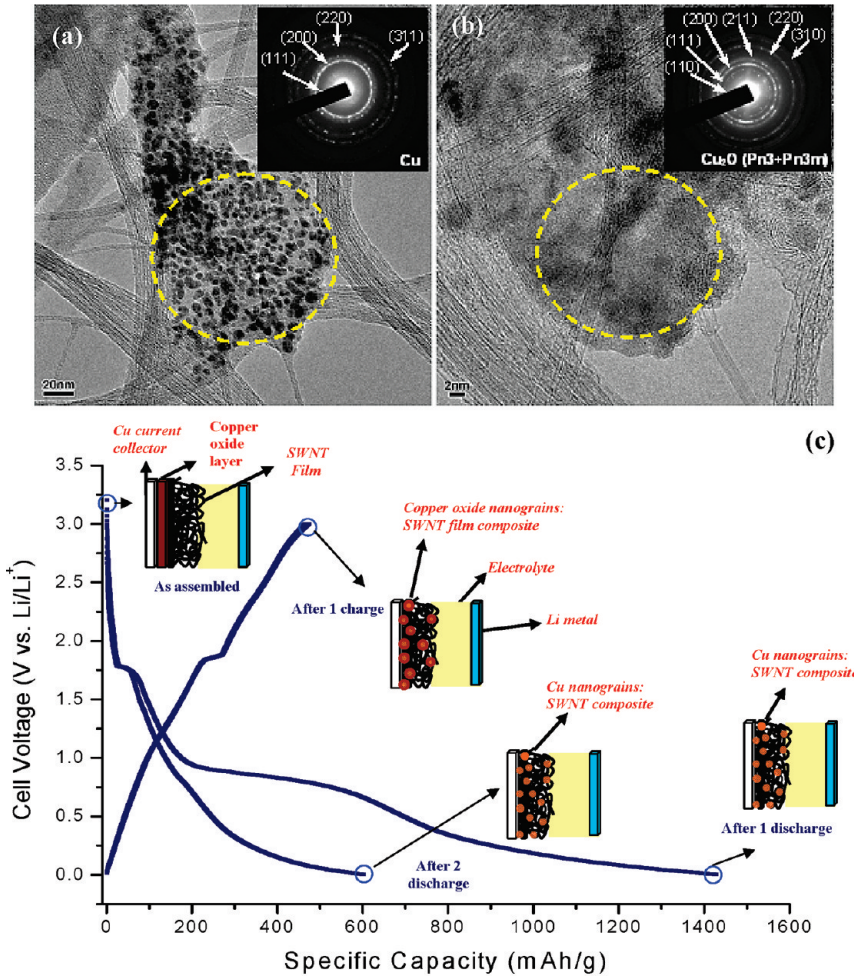

Figure 4. HRTEM images of purified SWNT film on heated Cu foil: (a) after 1st discharge; (b) after one complete cycle. The insets in panels a and b show the selected area electron diffraction (SAED) patterns recorded from the areas marked by the yellow circles. Cu nanoparticles are observed in the SWNT bundles after the first discharge cycle. Cu_2O nanoparticles are present in the SWNT bundles after one complete cycle. (c) First two charge−discharge cycles of the battery with the Cu/Cu_xO_y/SWNT sandwiched structure electrode. Schematic represent the Cu/SWNT film and Cu_xO_y/SWNT film composite formation in the battery at the end of each discharge and charge cycle. The Cu_xO_y present at the interface of the Cu and SWNT film in the as-assembled battery converts into Cu nanograins and forms a Cu/SWNT composite at the end of first discharge cycle. During the charging process, the Cu nanograins convert into Cu_2O nanograins and forms a copper oxide/SWNT film composite at the end of the charge cycle. This increases the conductivity of the Cu/Cu_xO_y/SWNT leading to a superior electrochemical performance compared to the battery with Cu/SWNT film.

The copper oxide formed at the interface of SWNT film and Cu foil exists as a thin film and it is very difficult to quantify the weight because of the *in situ* formation during the deposition of SWNT macrofilms. Hence, to give an idea on the contribution of copper oxide to the overall specific capacity of the system, the specific capacity was simply calculated with respect to the area of the electrode from the reversible 1.8 V plateau in the CV curves. In case 1, the capacity associated with the copper oxide in terms of the area is ~7 μAh/cm^2, while for the entire system it is ~48 μAh/cm^2. In the case of the heated Cu foil without SWNT macrofilm (case 4), the specific capacity was found to be ~9 μAh/cm^2, agreeing well with that calculated for the sandwiched composite. It appears that the contribution from the copper oxide is only about $^1/_7$ of the total capacity but may not be the true scenario based on the fact that the specific capacity is double or triple when the copper oxide is involved (Figure 3). The main reason for the increase in the specific capacity of the system may not be limited to the sole contribution from the redox reactions of copper oxide.

The existing composite structure is a mixture of a semiconducting and a highly electronic conducting system having a fine interface exhibiting a sandwiched structure. Li insertion capacity and the facile removal mainly depend on the diffusion or mobility of the Li ions in the host matrix. In the case of copper oxide, it has been reported that the insertion of Li ions has resulted in the decrease of the resistivity and the activation energy for the diffusion of ions drastically from 0.2 to 0.073 eV.[25] This is a favorable phenomenon for the increase in the amounts of Li ion insertion. As the Li ion insertion proceeds further, there is a predominant decrease

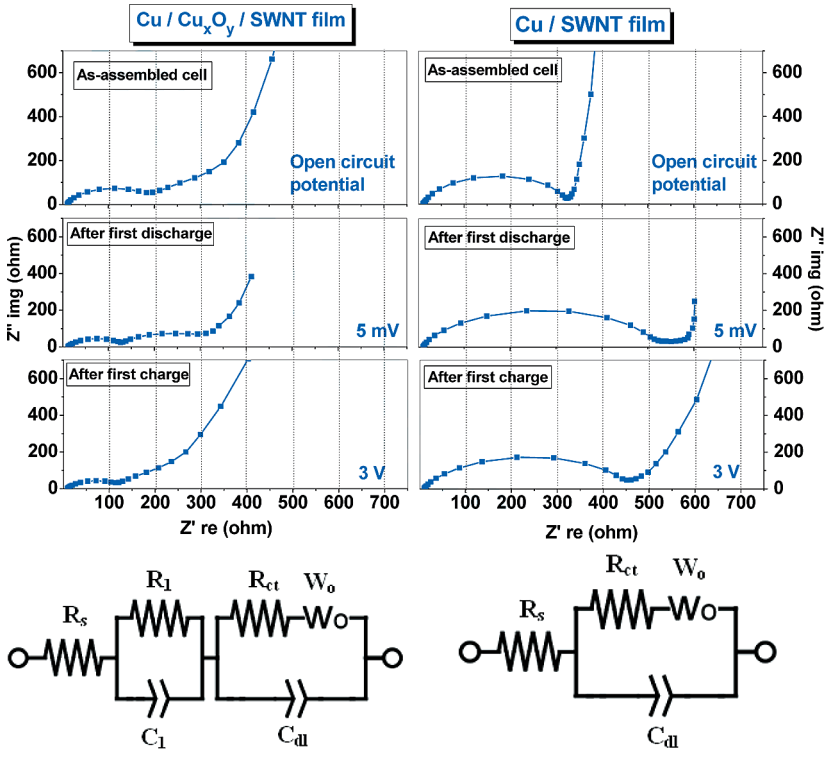

Figure 5. Electrochemical impedance spectroscopy measurements performed on the cells with the Cu/Cu$_x$O$_y$/SWNT sandwiched electrode and Cu/SWNT film electrode and their corresponding equivalent circuit model plots. The Nyquist spectra are measured in the frequency between 100 kHz to 10 mHz on the as-assembled cells at open circuit potential and during the first Li insertion and extraction process. The layered electrode structure with different type of materials gives two semicircles in the high and midfrequency region in the case of the battery with Cu/Cu$_x$O$_y$/SWNT electrode. The cell resistance of the battery with Cu/Cu$_x$O$_y$/SWNT sandwiched electrode is much lower than the cell with the Cu/SWNT film electrode, indicating a superior performance of the battery with the Cu/Cu$_x$O$_y$/SWNT sandwiched structures.

in the resistivity and the activation energy required for the Li ion diffusion which is mainly done by hopping mechanism. This is very important for an effective electron exchange reaction. Also, having a highly electronic conducting SWNT macrofilm over the copper oxide layer will enhance further the electron exchange reactions. In addition to the above reaction, during the electrochemical reaction of Li ions with CuO, the formation of metallic Cu nanoparticles (Figure 4a) has resulted in the formation of Li_2O and during the removal of Li ions, there is a formation of Cu_2O nanoparticles (Figure 4b) by the decomposition of Li_2O.[19] During this disproportion reaction, there is always oxygen evolution and the evolved oxygen is expected to be physiadsorbed by the SWNT macrofilm. It has been reported that the adsorption of oxygen by SWNT increases the electrical conductivity by at least 2 orders of magnitude.[26] This is an advantageous factor for the enhanced electrochemical performance of the system. This enhanced diffusion arising from the copper oxide and the improved electronic properties during the electrochemical insertion of Li ions has led to the high rate performance (50 C) of the sandwiched composite electrode. The aforementioned advantages are absent with respect to the Cu/SWNT film system where the capacity is much lower than the Cu/Cu$_x$O$_y$/SWNT sandwiched structure. The improved rate capability is also the virtue of the sandwiched composite where the diffusion of ions in the electrode is very important when the system is cycled at a high current.

The increase in the Li ion transfer rate across the electrolyte and the copper nanograins/SWNT composite system during the discharge−charge process is also evident from the electrochemical impedance measurements. The electrochemical impedance spectra measured from 100 kHz to 10 mHz on both the systems Cu/SWNT and Cu/Cu$_x$O$_y$/SWNT during the first lithium insertion−deinsertion cycle, and the typical Nyquist plots corresponding to the as-assembled cell impedance and the cells after a complete discharge and charge are shown in Figure 5 along with their corresponding RC equivalent circuit models based on the famous Randles circuit.[27] In the equivalent circuits, an intercept at the Z' real axis in the high frequency corresponds to the resistance of the electrolytes R_s. The semicircle in the middle frequency range indicates the charge transfer resistance R_{ct}, relating to the charge transfer through the electrode/electrolyte interface and the double layer capacitance C_{dl} formed due to the electrostatic charge separation near the electrode/electrolyte interface. Also, the inclined line in the low frequency represents the Warburg impedance W_o, which is related to solid-state diffusion of Li ions into the electrode material. The Nyquist plot of the Cu/SWNT film consisted of a high frequency semicircle and a low frequency spike at all voltages similar to that of a free-standing SWNT film.[13,28] However, for the Cu/Cu$_x$O$_y$/SWNT sandwiched electrode there are two semicircles in the high and middle frequency regions which can be explained by the additional circuit elements R_1 and C_1 in the equivalent circuit model as shown in Figure 5. The occurrence of the two semicircles can be attributed to the layered structure of the electrode with two different types of materials. The semicircle at the high frequency may be ascribed to the Li ion diffusion and charge separation at the Cu$_x$O$_y$/SWNT interface and the other semicircle in the mid-frequency is related to the regular charge transfer and double layer formation at the SWNT film/electrolyte interface.

The Nyquist spectra in Figure 5 indicate that as the intercalation level of Li ions increased, the electrical impedance of the cell with the Cu/Cu$_x$O$_y$/SWNT sandwiched electrode is much lower than that of the cell with the Cu/SWNT electrode at the end of the discharge

cycle. This is due to the formation of the Cu nanograin/SWNT composite (Figure 4c) during the Li insertion (discharge) process which reduced the charge transfer resistance significantly in the cell with the Cu/Cu_xO_y/SWNT electrodes. Also, as mentioned earlier, the possible evolution of the trace amount of oxygen due to the disproportionate reaction of CuO converting to Cu during the discharge and Cu converting into Cu_2O during the charging process is physisorbed by the SWNT macrofilms. It increases the conductivity of the SWNT macrofilm which leads to a much lower impedance of the cell with Cu/Cu_xO_y/SWNT electrode at the end of the charge cycle compared to that of the cell with Cu/SWNT electrode (Figure 5).

CONCLUSIONS

In summary, SWNT macrofilms were simply deposited on copper foils in CVD and a thin layer of copper oxide formed *in situ* at the current collector and the SWNT macrofilm interface. The resulted sandwiched structure consisting of nanotubes, metal, and metal oxide showed excellent reversibility and capacity as an anode material for Li ion battery applications. The sandwiched structure showed a remarkably high specific capacity at both low and high cycling currents. The reversible specific capacity at a cycling rate of 50 C was 220 mAh/g, which is extremely high for any carbon-based electrode material. The change in the electronic properties both in copper oxide and SWNT macrofilm during Li insertion−deinsertion was found to be responsible for such a high reversibility at high currents. The improvement in electrochemical performance has been addressed with a model involving a sandwiched composite structure, which can be extended to other metal oxides/CNT composites.

METHODS

Fabrication of the SWNT Macrofilms on Cu Foil. The macrofilms of carbon nanotubes were prepared *in situ* on copper foils by applying a liquid-free precursor system, where ferrocene/sulfur powders were mixed uniformly (atomic ratio Fe/S = 10:1) and as feedstock in a modified CVD system.[14] The growth was carried out at 1150 °C with a gas flow of argon (1500 mL/min) and hydrogen (150 mL/min) mixture.

Purification of SWNT Films. The SWNT films obtained from CVD were purified by first heating the films in air up to 450 °C for 1 h to remove amorphous carbon and then treated in 9 M HCl solution for 0.5 h to remove the iron catalyst particles.[17]

Estimation of the Weight of Active Material. Several copper electrodes from a bare copper foil were punched with a 0.5 in. diameter arch punch. The weight of each bare electrode is almost the same with less than 0.1 mg difference. After depositing the SWNT film on the copper foil by CVD, the electrodes were punched with the same 0.5 in. diameter arch punch and weighed. The weight of the bare copper electrode was subtracted from this weight to estimate the combined weight of the SWNT film and the copper oxide. Similar procedure was followed to estimate the weight of the purified SWNT films deposited on the heated copper foils.

Electrochemical Measurements. Two electrode test cells (Pred Materials) were used to assemble the batteries in a half cell configuration. The electrochemical characteristics were studied using galvanostatic charge−discharge cycling, electrochemical impedance spectroscopy, and cyclic voltammetry (CV). The galvanostatic cycling was performed at different rates ranging from 0.2 to 50 C, where the C-rate is based on the theoretical capacity of graphite (372 mAh/g) [Arbin Instruments, BT4, USA]. Cyclic voltammetry experiments were performed between 3.0 and 0.005 V at a scan rate, 0.05 mV/s. [Auto lab PGSTAT 30 (Echochemie, The Netherlands)]. The electrochemical impedance spectra were measured at frequencies in the range from 100 kHz to 10 mHz.

Acknowledgment. The financial support from National Science Foundation under the NSF award number CMMI #0753462 is gratefully acknowledged.

Supporting Information Available: XPS spectra of heated copper foil, galvanostatic charge discharge cycling of the batteries assembled in case 3 and case 4. This material is available free of charge *via* the Internet at http://pubs.acs.org.

REFERENCES AND NOTES

1. Armand, M.; Tarascon, J. M. Building Better Batteries. *Nature* **2008**, *451*, 652–657.
2. Tarascon, J. M.; Armand, M. Issues and Challenges Facing Rechargeable Lithium Batteries. *Nature* **2001**, *414*, 359–367.
3. Nagaura, T.; Tozawa, K. Lithium Ion Rechargeable Battery. *Prog. Batteries Solar Cells* **1990**, *9*, 209–217.
4. Chan, C. K.; Peng, H. L.; Liu, G.; Mcllwrath, K.; Zhang, X. F.; Huggins, R. A.; Cui, Y. High-Performance Lithium Battery Anodes Using Silicon Nanowires. *Nat. Nanotechnol.* **2008**, *3*, 31–35.
5. Taberna, P. L.; Mitra, S.; Poizot, P.; Simon, P.; Tarascon, J. M. High Rate Capabilities Fe_3O_4-Based Cu Nano-Architectured Electrodes for Lithium-Ion Battery Applications. *Nat. Mater.* **2006**, *5*, 567–573.
6. Dahn, J. R.; Zheng, T.; Liu, Y. H.; Xue, J. S. Mechanisms for Lithium Insertion in Carbonaceous Materials. *Science* **1995**, *270*, 590–593.
7. Sato, K.; Noguchi, M.; Demachi, A.; Oki, N.; Endo, M. A Mechanism of Lithium Storage in Disordered Carbons. *Science* **1994**, *264*, 556–558.
8. Idota, Y.; Kubota, T.; Matsufuji, A.; Maekawa, Y.; Miyasaka, T. Tin-Based Amorphous Oxide: A High-Capacity Lithium-Ion-Storage Material. *Science* **1997**, *276*, 1395–1397.
9. Poizot, P.; Laruelle, S.; Grugeon, S.; Dupont, L.; Tarascon, J. M. Nano-Sized Transition-Metal Oxides as Negative-Electrode Materials for Lithium-Ion Batteries. *Nature* **2000**, *407*, 496–499.
10. Gao, B.; Kleinhammes, A.; Tang, X. P.; Bower, C.; Fleming, L.; Wu, Y.; Zhou, O. Electrochemical Intercalation of Single-Walled Carbon Nanotubes with Lithium. *Chem. Phys. Lett.* **1999**, *307*, 153–157.
11. Raffaelle, R. P.; Landi, B. J.; Harris, J. D.; Bailey, S. G.; Hepp, A. F. Carbon Nanotubes for Power Applications. *Mater. Sci. Eng., B* **2005**, *116*, 233–243.
12. Morris, R. S.; Dixon, B. G.; Gennett, T.; Raffaelle, R.; Heben, M. J. High-Energy, Rechargeable Li-Ion Battery Based on Carbon Nanotube Technology. *J. Power Sources* **2004**, *138*, 277–280.
13. Ng, S. H.; Wang, J.; Guo, Z. P.; Wang, G. X.; Liu, H. K. Single Wall Carbon Nanotube Paper as Anode for Lithium-Ion Battery. *Electrochim. Acta* **2005**, *51*, 23–28.
14. Zhu, H. W.; Wei, B. Q. Direct Fabrication of Single-Walled Carbon Nanotube Macro-Films on Flexible Substrates. *Chem. Commun.* **2007**, *29*, 3042–3044.
15. Subramanian, V.; Zhu, H. W.; Wei, B. Q. High Rate Reversibility Anode Materials of Lithium Batteries from Vapor-Grown Carbon Nano-Fibers. *J. Phys. Chem. B* **2006**, *110*, 7178–7183.

16. Fong, R.; Vonsacken, U.; Dahn, J. R. Studies of Lithium Intercalation into Carbon Using Nonaqueous Electrochemical Cells. *J. Electrochem. Soc.* **1990**, *137*, 2009–2013.
17. Wei, J. Q.; *et al*. Ultrathin Single-Layered Membranes from Double-Walled Carbon Nanotubes. *Adv. Mater.* **2006**, *18*, 1695–1700.
18. Grugeon, S.; Laruelle, S.; Herrera-Urbina, R.; Dupont, L.; Poizot, P.; Tarascon, J. M. Particle Size Effects on the Electrochemical Performance of Copper Oxides toward Lithium. *J. Electrochem. Soc.* **2001**, *148*, A285–A292.
19. Debart, A.; Dupont, L.; Poizot, P.; Leriche, J. B.; Tarascon, J. M. A Transmission Electron Microscopy Study of the Reactivity Mechanism of Tailor-Made CuO Particles Toward Lithium. *J. Electrochem. Soc.* **2001**, *148*, A1266–A1274.
20. Zhang, D. W.; Yi, T. H.; Chen, C. H. Cu Nanoparticles Derived from CuO Electrodes in Lithium Cells. *Nanotechnology* **2005**, *16*, 2338–2341.
21. Morales, J.; Sanchez, L.; Martin, F.; Ramos-Barrado, J. R.; Sanchez, M. Nanostructured CuO Thin Film Electrodes prepared by Spray Pyrolysis: A Simple Method for Enhancing the Electrochemical Performance of CuO in Lithium Cells. *Electrochim. Acta* **2004**, *49*, 4589–4597.
22. Gao, X. P.; Bao, J. L.; Pan, G. L.; Zhu, H. Y.; Huang, P. X.; Wu, F.; Song, D. Y. Preparation and Electrochemical Performance of Polycrystalline and Single Crystalline CuO Nanorods as Anode Materials for Li Ion Battery. *J. Phys. Chem. B* **2004**, *108*, 5547–5551.
23. Wu, G. T.; Wang, C. S.; Zhang, X. B.; Yang, H. S.; Qi, Z. F.; Li, W. Z. Lithium Insertion into CuO/Carbon Nanotubes. *J. Power Sources* **1998**, *75*, 175–179.
24. Huang, H.; Kelder, E. M.; Schoonman, J. Graphite-Metal Oxide Composites as Anode for Li-Ion Batteries. *J. Power Sources* **2001**, *97−98*, 114–117.
25. Zheng, X. G.; Yamada, H.; Scanderbeg, D. J.; Maple, M. B.; Xu, C. N. Effect of Hole Doping in $Li_xCu_{1-x}O$. *Phys. Rev. B* **2003**, *67*, 214516.
26. Collins, P. G.; Bradley, K.; Ishigami, M.; Zettl, A. Extreme Oxygen Sensitivity of Electronic Properties of Carbon Nanotubes. *Science* **2000**, *287*, 1801–1804.
27. Randles, J. E. B. Kinetics of Rapid Electrode Reactions. *Discuss. Faraday Soc.* **1947**, *1*, 11–19.
28. Claye, A. S.; Fischer, J. E.; Huffman, C. B.; Rinzler, A. G.; Smalley, R. E. Solid-State Electrochemistry of the Li Single Wall Carbon Nanotube System. *J. Electrochem. Soc.* **2000**, *147*, 2845–2852.